Hydrogen desorption from Si: How does this relate to film growth?

C. Michael Greenlief[a] and Michael Armstrong
Department of Chemistry, University of Missouri–Columbia, Columbia, Missouri 65211

(Received 10 January 1995; accepted 10 April 1995)

The desorption of hydrogen from the Si(100) surface is investigated. The hydrogen coverage is generated by the adsorption of atomic hydrogen, by the thermal decomposition of disilane, or during silicon epitaxy using silane in a rapid thermal chemical vapor deposition reactor. Temperature programmed desorption studies are then used to help yield information about the hydrogen surface coverage and the desorption kinetics of hydrogen. The desorption order of hydrogen is first order, consistent with previously reported single crystal studies. However, the activation energy for desorption of hydrogen from surfaces generated during Si epitaxy with SiH_4 is considerably different. The activation energy for hydrogen desorption from these epitaxially grown layers is 49 ± 3 kcal/mol. The presence of monatomic steps on the surface, which are created during the temperature quench, is believed to play a role in this difference of activation energies. Single crystal, ultra-high vacuum based studies using atomic hydrogen and disilane adsorption and desorption are used to gain further insight into this phenomena. © *1995 American Vacuum Society.*

I. INTRODUCTION

The interaction of hydrogen with silicon has been investigated over a number of years. Early studies focused on the adsorption of hydrogen and how it could alter the electronic structure of silicon.[1,2] More recently, the desorption of hydrogen from Si has received considerable attention. The recombinative desorption of hydrogen was assumed to be a second order process in early temperature programmed desorption (TPD) studies.[3] This process was believed to be analogous to hydrogen desorption from metal surfaces. However, Shinniah *et al.*[4,5] clearly showed by laser-induced thermal desorption (LITD) that the recombinative desorption of hydrogen from the Si(100) surface was a first order process. This surprising result generated a number of other investigations. A recent literature search revealed that there are now well over 90 published reports dealing with various aspects of hydrogen desorption from silicon.[6]

Understanding the interactions of hydrogen with the silicon surface is also needed for a mechanistic interpretation of the chemical vapor deposition (CVD) of silicon from silanes.[7] Hydrogen at the Si surface during epitaxy can limit the adsorption of silane and therefore affect the Si growth rate. The desorption of H_2 frees sites on the surface which then allow for additional SiH_4 adsorption and reaction. There is a balance between adsorption and reaction of silane with hydrogen desorption that governs the overall Si growth rate.

The adsorption of hydrogen on the Si(100)-(2×1) surface and the dynamics of its desorption were calculated by a number of investigators[8–17] in an effort to help explain this phenomena. The structure of the monohydride phase,[8–10] the Si–H bond strength,[11] the activation energy for desorption of H_2,[12] and the mechanism leading to desorption[13–17] were all examined in these theoretical studies. The kinetics of the H_2 desorption process and its dynamics were also determined by several research groups with a variety of experimental methods.[4,5,18–31]

In this article, hydrogen TPD results from a number of different samples, heating rates, and coverages are examined. The hydrogen surface coverage ranges from 0.1 to 1 ML (1 ML$=6.8\times10^{14}$ Si atoms cm^{-2}). Over this coverage range, the desorption kinetics of hydrogen are known to be first order and independent of coverage.[4,5,19,23] The TPD results are examined by a variety of analysis methods in order to make sure that the kinetic parameters obtained are not unique to the analysis method. Atomic hydrogen, silane, and disilane are used as the chemical sources for surface hydrogen.

II. EXPERIMENT

The experiments described in this article are performed in two separate systems. The film growth studies are performed in a rapid thermal chemical vapor deposition (RTCVD) reactor that is coupled to a differentially pumped quadrupole mass spectrometer. This system is described in detail elsewhere.[32] The Si samples are heated by a set of infrared lamps and the temperature of the substrate is monitored by an optical pyrometer.

The samples in the RTCVD reactor are double-sided polished 3.25 in. Si(100) wafers (*n*-type, Sb doped, 10 mΩ-cm resistivity). The wafers are RCA and HF cleaned prior to loading into the reactor. The sample is outgassed at 573 K followed by a brief anneal to 1000 K. The sample temperature is then lowered to the desired growth temperature and silane (Airco, ultra large scale integrated grade) flow is established.

The second experimental system is a stainless steel ultrahigh vacuum (UHV) chamber that is described elsewhere.[33] The base pressure of the system is 6×10^{-11} Torr with a typical working pressure of 1×10^{-10} Torr. The chamber is equipped with a double-pass cylindrical mirror analyzer (CMA) for Auger electron and photoelectron spectroscopies, a differentially pumped ultraviolet discharge lamp, twin x-ray source, ion gun, and quadrupole mass spectrometer for both temperature programmed desorption and secondary ion mass spectrometry.

[a]Author to whom correspondence should be addressed.

 ©1995 American Vacuum Society

Samples that are used in the UHV chamber are cleaved into 10×25×0.4 mm rectangles from *n*-type Si(100) wafers [Virginia Semiconductor, ±0.25° of the (100) plane, Sb doped, 5–10 mΩ-cm resistivity] and mounted to a liquid nitrogen cooled manipulator. The sample is held by molybdenum clamps for resistive heating. The sample temperature is monitored by a pair of chromel-alumel thermocouples attached to the back of the sample with Aremco 516 ceramic adhesive.

Surface cleanliness is followed by Auger electron and ultraviolet photoelectron spectroscopies. A clean surface is generated by the removal of the native oxide by repeated heating to 1213 K in vacuum followed by slow cooling to room temperature.

Disilane and atomic hydrogen are the two hydride sources used in the UHV chamber. Disilane (Voltaix, ultrahigh purity grade, minimum purity 99.998%) is further purified by several freeze-pump-thaw degassing cycles. Hydrogen (Linde, prepurified grade, minimum purity 99.99%) is used directly after passing the gas through a liquid nitrogen cooled trap. The purity of the gases is also checked *in situ* by mass spectrometry. Atomic hydrogen is generated by flowing hydrogen gas over a hot tungsten filament in line-of-sight of the silicon surface.

III. RESULTS

A. UHV studies

The H_2 TPD results from the decomposition of Si_2H_6 are shown as Figure 1. The silicon surface temperature was 110 K during the Si_2H_6 exposures and the temperature ramp rate was 6 K s^{-1}. At low Si_2H_6 exposures (Fig. 1a), a single desorption state is observed near 800 K. This desorption state has been previously identified as β_1 by Schulze and Henzler.[3] Increasing the Si_2H_6 exposure results in the saturation of the β_1 state and a new desorption state (β_2) starts to populate at lower temperatures. The β_2 state also saturates for coverages greater than 2.3×10^{14} Si_2H_6 moleules cm^{-2}.

The data from Fig. 1 and several other replicate sets of data were analyzed to determine the activation energy for desorption and the preexponential factor that govern the kinetics of the β_1 state. Analysis of the thermal desorption data by the leading edge or threshold TPD method (TTPD)[34,35] was performed. This method uses an Arrhenius plot of the desorption rate versus temperature. The slope of the plot is related to the activation energy for desorption and the y-intercept is the natural log of the preexponential factor. This analysis method is used for all the hydrogen desorption results with initial hydrogen atom coverages less than 2 $\times10^{-14}$ cm^{-2}. The results of this analysis method are summarized in Table I.

The data are also analyzed by the Chan, Aris, and Weinberg method (CAW).[38] This method depends on knowledge of the ramp rate, peak temperature, and peak width at 1/2 and 3/4 maximum. The results of this analysis method are listed in Table I.

The β_1 desorption state was also simulated by kinetic modeling. Figure 2 shows the results of a typical fit to the

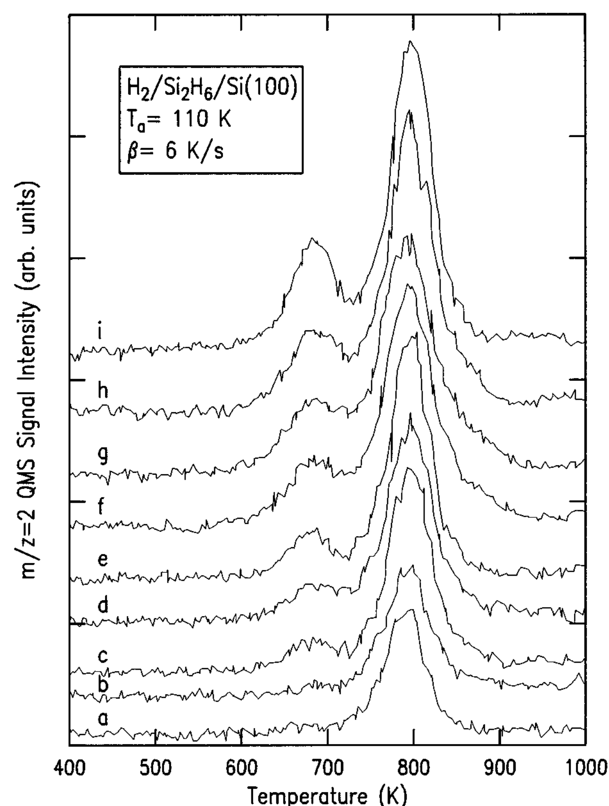

FIG. 1. H_2 thermal desorption spectra for several coverages of Si_2H_6. The temperature ramp rate was 6 K s^{-1} and the adsorption temperature was 110 K. The Si_2H_6 coverages shown are (a) 2.4×10^{13}, (b) 2.5×10^{13}, (c) 5.0×10^{13}, (d) 5.4×10^{13}, (e) 5.8×10^{13}, (f) 7.4×10^{13}, (g) 8.1×10^{13}, (h) 8.3×10^{13}, and (i) 8.7×10^{13} Si_2H_6 molecules cm^{-2}.

experimental data used in determining the hydrogen desorption kinetics using the kinetic model. The solid line is the desorption trace for hydrogen resulting from the decomposition of disilane for an initial disilane coverage of 5.0 $\times10^{-13}$ molecules cm^{-2}. The dashed line shows the results of the simulated TPD spectrum. For this fit, an activation energy of 53.5 kcal mol^{-1} and a preexponential factor of 1×10^{14} s^{-1} are used. There is excellent agreement between the two spectra. The agreement between the experi-

TABLE I. Kinetic parameters for the desorption of hydrogen from Si(100)

Hydride source	Data analysis method	E_a (kcal mol^{-1})	ν (s^{-1})
H atoms	TTPD[a]	57±1	$(6\pm2)\times10^{14}$
	CAW[b]	57±3	$(7\pm5)\times10^{15}$
	Simulation	58±2	$(2\pm2)\times10^{15}$
Si_2H_6	TTPD	54±2	$(2\pm4)\times10^{12}$
	CAW	53±1	$(6\pm5)\times10^{14}$
	Simulation	53.1±1	$(9\pm2)\times10^{13}$
SiH_4	RLK[c]	45±2	$(1\pm1)\times10^{12}$
	TTPD	50±4	$(3\pm4)\times10^{9}$
	CAW	48±1	$(3\pm6)\times10^{14}$
	Simulation	48.5±1	$(6\pm4)\times10^{12}$

[a]References 34 and 35.
[b]Reference 36.
[c]Reference 37 and 38.

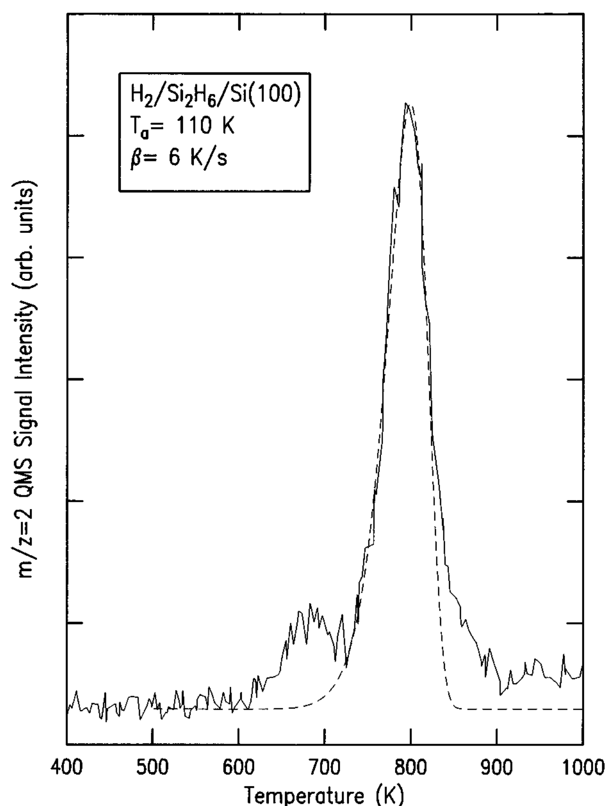

FIG. 2. *Solid line*: H_2 TPD spectrum for an initial disilane coverage of 5.0×10^{13} Si_2H_6 molecules cm^{-2}. The adsorption temperature is 110 K and the ramp rate is 6 K s^{-1}. *Dashed line*: Computer fit of the high temperature desorption state. The activation energy used for the fit is 53.5 kcal mol^{-1} and the preexponential factor is 1×10^{14} s^{-1}.

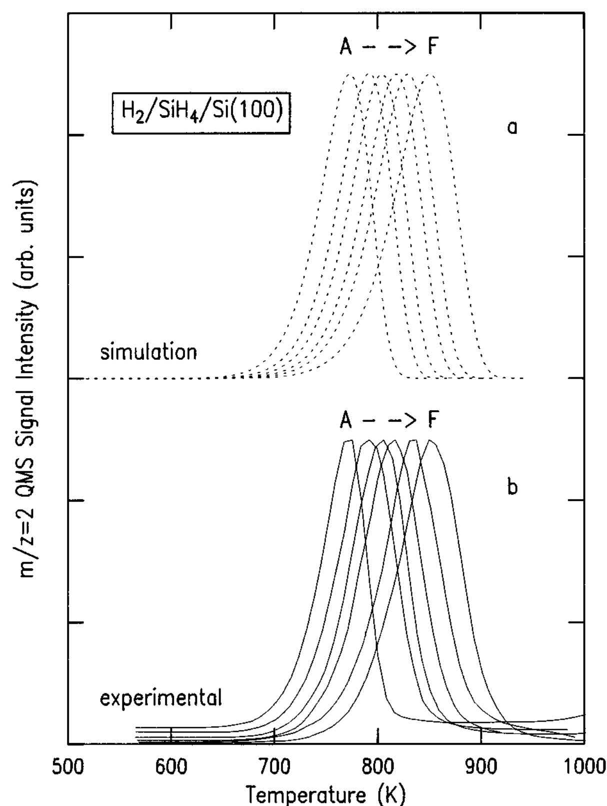

FIG. 3. a: *upper panel*, simulated TPD spectra for the same coverages and ramp rates used in part a. The activation energy for desorption used in the simulations is 48.5 kcal mol^{-1} and the preexponential factor used is 6 $\times10^{12}$ s^{-1}. b: *lower panel*, TPD spectra for the desorption of H_2 from Si(100) at several different ramp rates. The initial hydrogen coverage is 5.4×10^{14} cm^{-2}. The ramp rates shown are A) 2.8, B) 6.3, C) 10.3, D) 17.9, E) 27.7, and F) 60.8 K s^{-1}.

mental and calculated spectra was consistently of this quality. The entire set of data is fit with an activation energy of 53.1 ± 1 kcal mol^{-1} and a preexponential factor of $(9\pm2)\times10^{13}$ s^{-1}. These kinetic parameters are averaged over the entire range of coverages used in this study and the kinetic parameters do not exhibit any unusual coverage dependence.

Atomic hydrogen was also used as a hydride source. Hydrogen atoms were exposed to Si(100) at a surface temperature of 110 K. Thermal desorption spectra were obtained as a function of exposure. The H_2 TPD spectra were very similar to those presented in Figure 1. The only significant difference was that the desorption peak width of the β_1 state was narrower. The desorption order of hydrogen when using atomic hydrogen as the hydride source was first order. The activation energy for desorption and preexponential factor determined by computer modeling was 58 ± 2 kcal mol^{-1} and $(2\pm2)\times10^{15}$ s^{-1}, respectively, and are included in Table I.

The error limits for the activation energies and preexponential factors listed in Table I are the result of both the experimental deviations (one experiment to the next) and systematic errors in the analysis method. For example, in the CAW method, improper determination of the peak width at 1/2 or 3/4 maximum can lead to about an order of magnitude change in the preexponential factor. The error limits are listed for one standard deviation. All the experimental data are analyzed by the CAW method and by computer simulation. However, only a portion of the data are analyzed by the TTPD method.

B. RTCVD studies

A set of thermal desorption experiments completed in the RTCVD system are shown in Figure 3. The lower portion of the figure shows TPD spectra obtained at several different ramp rates. The hydrogen coverage is generated by the decomposition of SiH_4. A Si(100) wafer is exposed to a SiH_4 flow rate of 3 mTorr for 5 min at a surface temperature of 813 K to establish equilibrium growth conditions, followed by quenching of the gas flow and temperature to freeze-out the hydrogen coverage.[32] The hydrogen coverage shown for each spectrum in Figure 3 is 5.4×10^{14} cm^{-2}. Figure 3a is the TPD spectrum obtained with a ramp rate of 2.8 K s^{-1}. As the ramp rate is increased from 2.8 to 60.8 K s^{-1}, the peak temperature also increases.

The upper portion of Figure 3 is a set of simulated TPD spectra using the same ramp rates as the experimental data presented in the lower portion of the figure. These spectra are calculated using an activation energy of 48.5 kcal mol^{-1} and a preexponential factor of 6 $\times$ 10^{12} s^{-1}. The desorption

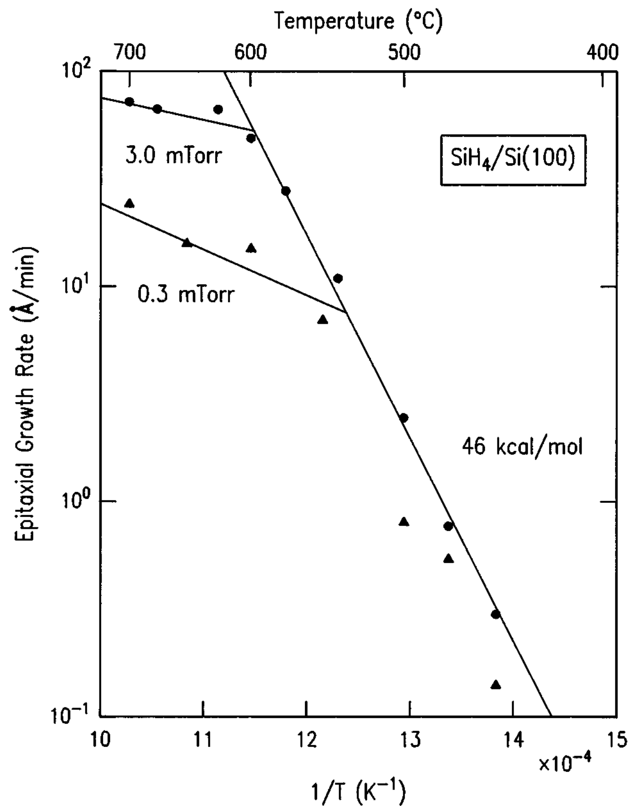

FIG. 4. Growth rates for epitaxial silicon on Si(100) from SiH_4. Two growth conditions are shown: 3 mTorr (solid circles) and 0.3 mTorr (solid triangles). The activation energy shown is determined from a least-squares fit to the data between 400 and 600 °C at a pressure of 3 mTorr. The film thicknesses were determined by seconday-ion-mass spectroscopy.

peak temperatures for the simulated spectra match closely with the experimentally determined results. The poorest fit is with the fastest ramp rate used (60.8 K s^{-1}) where the simulated peak temperature is 5 K lower than the measured spectrum. The leading edge of each desorption peak is reproduced well and, in most cases, the width of the calculated peaks are in good agreement with the measured spectra. The entire set of thermal desorption spectra can be simulated (both peak temperature and width) by an activation energy for desorption of 48.5±1 kcal mol^{-1} and a preexponential factor of $(6\pm4)\times10^{12}$ s^{-1}.

The rate data shown in Figure 3 was also analyzed by examining the peak temperature shift as a function of ramp rate,[37,38] in addition to the CAW method. The results of these analyses are included in Table I.

Figure 4 shows an Arrenhius plot of the silicon growth rate from silane on Si(100) at two different SiH_4 flow rates in the RTCVD reactor. The film thickness was determined by secondary ion mass spectrometry (SIMS) in a CAMECA-4f. The Sb doping of the substrate was used to derive the layer thickness. Two distinct growth regimes are observed. These two regimes have been previously identified.[39] The higher activation energy regime is observed at temperatures below 550 °C, is independent of silane flow rate, and is attributed to Si growth that is limited by the desorption of hydrogen from the growing surface. The high temperature regime has a significantly lower activation energy, is dependent on SiH_4 flow rate, and is attributed to Si growth that is limited by SiH_4 adsorption.

TABLE II. Comparison of kinetic parameters for H_2 desorption from Si(100).

Hydride source	Reference	Experimental method	E_a (kcal mol^{-1})	ν (s^{-1})
H atoms	23	SHG[a]	57.2	2.1×10^{15}
	5	LITD[b]	45±2	2.2×10^{11}
	19	LITD	58±2	$(5.5\pm5)\times10^{15}$
	18	TPD[c]	57	2.0×10^{15}
	20	LITD	57.2±2.6	$2.21\times10^{15\pm1}$
	This study	TPD	57.5±2	$(3\pm3)\times10^{15}$
Si_2H_6	20	LITD	54.3±2.3	$2.32\times10^{14\pm1}$
	This study	TPD	53±2	$(1\pm3)\times10^{14}$
SiH_4	This study	TPD	49±3	$8\times10^{13\pm1}$

[a]SHG: second harmonic generation.
[b]LITD: laser induced thermal desorption.
[c]TPD: temperature programmed desorption.

Table II is a comparison of the H_2 desorption kinetic parameters obtained in this study. Also shown are the desorption kinetic parameters of H_2 from Si(100) when using atomic hydrogen or disilane as a hydride source from previous studies. There is excellent agreement between the various research groups for the activation energy and preexponential factor for H_2 desorption when using disilane and atomic hydrogen in the UHV studies. However, the kinetic parameters obtained with silane in the stop/growth RTCVD studies are significantly different. Both the activation energy for desorption and the preexponential factor are lower.

IV. DISCUSSION

The activation energies and preexponential factors obtained from the different analysis methods used in this study are compared in Table I. The first point to note is that the TPD results analyzed by this variety of methods does lead to a set of kinetic parameters that are reasonably close with one another. This result shows that the kinetic parameters obtained are not dependent on the analysis method used. The parameters listed in Table II from this study are obtained by averaging over the entire set of data, regardless of the analysis method. Therefore, the average is weighted some by the CAW and computer simulation determinations since all of the data are analyzed by these two methods and only the low coverage data are analyzed by the TTPD method.

Table II compares the kinetic parameters from this study with those previously obtained in the literature. The activation energy for desorption of H_2 when using atomic H as the hydride source obtained here is in excellent agreement with other investigators' values (with the exception of Ref. 5). The same type of agreement is obtained with disilane as the hydride precursor. Silane seems to be the only exception. The hydrogen coverage with silane is generated when the molecule decomposes on the surface. This is a process that also deposits Si onto the original substrate. The hydrogen coverage from silane is generated by interrupting the growth process. High-resolution transmission electron microscopy revealed that the Si film is epitaxial. However, since the films

in TPD studies are not annealed to remove the hydrogen, it is expected that the atomic level structure of the outermost layer is not complete. In other words, there is a partial Si layer on top of the substrate. This structure can be thought of as an atomically rough surface. The rough structure can be contrasted with the experiments performed on well-annealed and atomically smooth single crystal studies in UHV. The difference in the local structure for the ''rough'' surfaces may account for the difference in the kinetic parameters obtained here; a lower activation energy for desorption and a lower preexponential.

In a series of papers, Zare and co-workers[28–30] demonstrated that the internal energy distribution for hydrogen desorption was the same whether atomic hydrogen or disilane was used as the hydrogen source. It is plausible that the hydrogen internal state distribution with SiH_4 as the hydrogen source is the same or very similar to the atomic hydrogen and disilane case. The studies by Zare and co-workers clearly show that the recombinative desorption of hydrogen from Si(100) occurs through a common intermediate. However, the authors did not examine closely the desorption kinetics which could be different.

In a recent study,[20] George and co-workers measured the desorption kinetics of hydrogen from the decomposition of disilane. This study was undertaken to test whether disilane could atomically roughen a Si(100) surface in an UHV environment and lower the desorption energy of H_2. They concluded that there was no difference in the activation energy for desorption of hydrogen when using either atomic hydrogen or disilane as the hydrogen source. Using the root-mean-squared displacement of a silicon adatom at 600 K,[40,41] they were able to show that Si could diffuse easily to form islands prior to H_2 desorption and thereby removing any atomic-level roughness induced by the adsorption of disilane. The activation energy for H_2 desorption from the decomposition of disilane we obtained here is only slightly less than that for the activation energy obtained with atomic H. This result confirms that the roughness is removed prior to desorption of hydrogen in these UHV experiments.

The activation energy for the growth rate of Si on Si(100) from the decomposition of SiH_4 is 46 kcal mol^{-1} for the temperature range of 425–550 °C and a pressure of 3 mTorr.[39] Over this temperature range the growth rate is limited by the desorption of hydrogen. The activation energy for Si growth is within the experimental error of the activation energy measured for desorption of hydrogen from SiH_4 decomposition. The atomic level structure of the film during growth should be similar to that in our desorption studies since we are just quenching the reaction. The similarity of the two activation energies suggests that the quenching experiments are monitoring more closely the local growth environment than are the desorption experiments conducted in UHV even though desorption may be occurring through a common intermediate. This result, taken with the disilane resutls, implies that the outermost growing layer during epitaxy may involve a roughness extended over several atomic layers.

V. CONCLUSIONS

The desorption of hydrogen from the Si(100) surface is a first order process that is independent of the hydride source. The activation energy for desorption of hydrogen when using atomic H or disilane as the hydrogen precursor is almost the same. However, when silane is used in the stop/growth CVD studies, the activation energy for hydrogen desorption is lowered. The activation energy of 49 ± 3 kcal mol^{-1} is the same as the activation energy for Si growth between 700 and 840 K. This result shows that the growth process in this temperature range is limited by the desorption of hydrogen. Kinetic modeling of silicon growth from silane should take into account these differences in the kinetic parameters.

ACKNOWLEDGMENTS

The authors wish to thank Professor S. George and Dr. M. Liehr for a number of stimulating discussions. The authors gratefully acknowledge the National Science Foundation (Grant No. CHE-9357133) for support of this research. One of the authors (C.M.G.) also acknowledges the National Science Foundation for a Young Investigator Award.

[1]R. Butz, E. M. Oellig, H. Ibach, and H. Wagner, Surf. Sci. **147**, 343 (1984).
[2]F. J. Himpsel and D. E. Eastman, J. Vac. Sci. Technol. **16**, 1297 (1979).
[3]G. Schulze and M. Henzler, Surf. Sci. **124**, 336 (1983).
[4]K. Sinniah, M. G. Sherman, L. B. Lewis, W. H. Weinberg, J. T. Yates, Jr., and K. C. Janda, Phys. Rev. Lett. **62**, 567 (1989).
[5]K. Sinniah, M. G. Sherman, L. B. Lewis, W. H. Weinberg, J. T. Yates, Jr., and K. C. Janda, J. Chem. Phys. **92**, 5700 (1990).
[6]The literature search included papers abstracted prior to December 31, 1994.
[7]J. M. Jasinski, B. S. Meyerson, and B. A. Scott, Annu. Rev. Phys. Chem. **38**, 109 (1987).
[8]J. A. Appelbaum and D. R. Hamann, in *Theory of Chemisorption*, edited by J. R. Smith (Springer, Berlin, 1980), p. 43 and references therein.
[9]X. M. Zheng and P. V. Smith, Surf. Sci. **279**, 127 (1992).
[10]T. Uchiyama and M. Tsukada, Surf. Sci. **295**, L1037 (1993).
[11]P. Nachtigall, K. D. Jordan, and K. C. Janda, J. Chem. Phys. **95**, 8652 (1991).
[12]Z. Jing and J. L. Whitten, J. Chem. Phys. **98**, 7466 (1993).
[13]C. J. Wu, I. V. Ionova, and E. A. Carter, Surf. Sci. **295**, 64 (1993); C. J. Wu and E. A. Carter, Chem. Phys. Lett. **185**, 172 (1991).
[14]Y. L. Yang and M. P. D'Evelyn, J. Vac. Sci. Technol. A **11**, 2200 (1993); M. P. D'Evelyn, Y. L. Yang, and L. F. Sutcu, J. Chem. Phys. **96**, 852 (1992).
[15]P. Nachtigall, K. D. Jordan, and C. Sosa, J. Chem. Phys. **101**, 8073 (1994).
[16]Z. Jing and J. L. Whitten, Phys. Rev. B **48**, 17296 (1993); Z. Jing, G. Lucovsky, and J. L. Whitten, Surf. Sci. **296**, L33 (1993); Z. Jing and J. L. Whitten, Phys. Rev. B **46**, 9544 (1992).
[17]J. Sheng and J. Z. H. Zhang, J. Chem. Phys. **97**, 596 (1992).
[18]M. C. Flowers, N. B. H. Jonathan, Y. Liu, and A. Morris, J. Chem. Phys. **99**, 7038 (1993).
[19]M. L. Wise, B. G. Koehler, P. Gupta, P. A. Coon, and S. M. George, Surf. Sci. **258**, 166 (1991).
[20]L. A. Okada, M. L. Wise, and S. M. George, Appl. Surf. Sci. **82/83**, 410 (1994).
[21]C. M. Greenlief, S. M. Gates, and P. A. Holbert, J. Vac. Sci. Technol. A **7**, 1845 (1989).
[22]C. M. Greenlief and M. Liehr, Appl. Phys. Lett. **64**, 601 (1994).
[23]U. Höfer, L. Li, and T. F. Heinz, Phys. Rev. B **45**, 9485 (1992).
[24]K. W. Kolasinski, W. Nessler, A. de Meijere, and E. Hasselbrink, Phys. Rev. Lett. **72**, 1356 (1994).
[25]K. W. Kolasinski, W. Nessler, K.-H. Bornscheuer, and E. Hasselbrink, J. Chem. Phys. **101**, 7082 (1994).
[26]K. W. Kolasinski, S. F. Shane, and R. N. Zare, J. Chem. Phys. **96**, 3995 (1992).

[27]S. F. Shane, K. W. Kolasinski, and R. N. Zare, J. Chem. Phys. **97**, 1520 (1992).
[28]S. F. Shane, K. W. Kolasinski, and R. N. Zare, J. Chem. Phys. **97**, 3704 (1992).
[29]Y. -S. Park, J. -Y. Kim, and J. Lee, J. Chem. Phys. **98**, 757 (1993).
[30]K. Ueda, S. Kodama, and A. Takano, Vacuum **43**, 795 (1992).
[31]W. R. Wampler, S. M. Myers, and D. M. Follstaedt, Phys. Rev. B **48**, 4492 (1993).
[32]M. Liehr, C. M. Greenlief, M. Offenberg, and S. R. Kasi, J. Vac. Sci. Technol. A **8**, 2960 (1990).
[33]C. M. Greenlief and D. A. Klug, J. Phys. Chem. **96**, 5424 (1992).
[34]E. Habenschaden and J. Küppers, Surf. Sci. **138**, L147 (1984).
[35]J. B. Miller, H. R. Siddiqui, S. M. Gates, J. N. Russell, Jr., J. T. Yates, Jr., J. C. Tully, and M. J. Cardillo, J. Chem. Phys. **87**, 6725 (1987).
[36]C.-M. Chan, R. Aris, and W. H. Weinberg, Appl. Surf. Sci. **1**, 360 (1978).
[37]P. A. Redhead, Vacuum **12**, 203 (1962).
[38]F. M. Lord and J. S. Kittelberger, Surf. Sci. **43**, 173 (1974).
[39]M. Liehr, C. M. Greenlief, S. R. Kasi, and M. Offenberg, Appl. Phys. Lett. **56**, 629 (1990).
[40]Y. Mo, J. Kleiner, M. B. Webb, and M. G. Lagally, Phys. Rev. Lett. **66**, 1998 (1991).
[41]Y. Mo, J. Kleiner, M. B. Webb, and M. G. Lagally, Surf. Sci. **268**, 275 (1992).